Article

Hydrogen Encapsulation in a Silicon Clathrate Type I Structure: Na(H)Si: Synthesis and Characterization

Doinita Neiner, Norihiko L. Okamoto, Cathie L. Condron, Quentin M. Ramasse, Ping Yu, Nigel D. Browning, and Susan M. Kauzlarich

J. Am. Chem. Soc., **2007**, 129 (45), 13857-13862• DOI: 10.1021/ja0724700 • Publication Date (Web): 24 October 2007

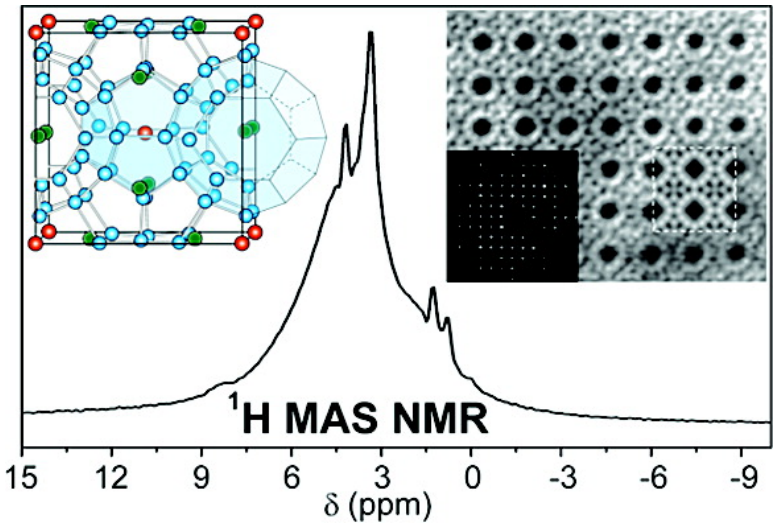

More About This Article

Additional resources and features associated with this article are available within the HTML version:

- Supporting Information
- Links to the 3 articles that cite this article, as of the time of this article download
- Access to high resolution figures
- Links to articles and content related to this article
- Copyright permission to reproduce figures and/or text from this article

View the Full Text HTML

J|A|C|S
ARTICLES
Published on Web 10/24/2007

Hydrogen Encapsulation in a Silicon Clathrate Type I Structure: $Na_{5.5}(H_2)_{2.15}Si_{46}$: Synthesis and Characterization

Doinita Neiner,[†] Norihiko L. Okamoto,[‡] Cathie L. Condron,[†] Quentin M. Ramasse,[§] Ping Yu,[||] Nigel D. Browning,[‡,⊥] and Susan M. Kauzlarich*,[†]

Contribution from the Department of Chemistry, Department of Chemical Engineering and Materials Science, and NMR Facility, One Shields Ave, University of California, Davis, California 95618, National Center of Electron Microscopy, Lawrence Berkeley Laboratory, 1 Cyclotron Rd, Berkeley, California 94270, and Materials Science and Technology Division, Lawrence Livermore National Laboratory, Livermore, California 94550

Received April 9, 2007; E-mail: smkauzlarich@ucdavis.edu

Abstract: A hydrogen-encapsulated inorganic clathrate, which is stable at ambient temperature and pressure, has been prepared in high yield. $Na_{5.5}(H_2)_{2.15}Si_{46}$ is a sodium-deficient, hydrogen-encapsulated, type I silicon clathrate. It was prepared by the reaction between NaSi and NH_4Br under dynamic vacuum at 300 °C. The Rietveld refinement of the powder X-ray diffraction data is consistent with the clathrate type I structure. The type I clathrate structure has two types of cages where the guest species, in this case Na and H_2, can reside: a large cage composed of 24 Si, in which the guest resides in the *6d* crystallographic position, and a smaller one composed of 20 Si, in which the guest occupies the *2a* position. Solid-state ^{23}Na, ^{1}H, and ^{29}Si MAS NMR confirmed the presence of both sodium and hydrogen in the clathrate cages. ^{23}Na NMR shows that sodium completely fills the small cage and is deficient in the larger cage. The ^{1}H NMR spectrum shows a pattern consistent with mobile hydrogen in the large cage. ^{29}Si NMR spectrum is consistent with phase pure type I clathrate framework. Elemental analysis is consistent with the stoichiometry $Na_{5.5}(H_{2.15})_2Si_{46}$. The sodium occupancy was also examined using spherical aberration (Cs) corrected scanning transmission electron microscopy (STEM). The high-angle annular dark-field (HAADF) STEM experimental and simulated images indicated that the Na occupancy of the large cage, *6d* sites, is less than 2/3, consistent with the NMR and elemental analysis.

Introduction

One of today's grand energy challenges is the reduction of the use of fossil fuels and the replacement of that with alternative energy sources. One such energy source is hydrogen.[1] Hydrogen is an ideal substitute for fossil fuels, but there are a number of barriers related to hydrogen production, transportation, storage, and technology that need to be overcome to facilitate its use. There has been a great deal of interest in the development of reversible systems for hydrogen storage. One simple solution is to develop micro- or mesoporous materials that can uptake hydrogen molecules in their cavities. The hydrogen molecules are forced into the cavities at low temperatures and high pressures and they can be released by raising the temperature.[2,3] Microporous materials such as metal organic frameworks (MOFs), zeolites, and porous carbon are compounds with high surface area and therefore have received increasing attention due to their potential use in hydrogen storage applications.[4,5] Of the porous materials proposed as hydrogen adsorbents at cryogenic temperatures, MOFs have received significant attention. MOFs have been reported to adsorb up to 7.5% (wt) hydrogen at 77 K under ~70 bar hydrogen pressure.[6,7] Additionally, Zeolites have been reported to have a hydrogen storage capacity up to 4.5% (wt) at 77 K.[8,9] Carbon-based materials such as porous carbon and single-wall nanotubes which can adsorb hydrogen at 77 K and ~80 atm up to 8%[10] have received particular attention. However, there is significant controversy over some of the initial results.[11]

Another class of materials that show hydrogen adsorption capabilities are clathrate hydrates.[12] Gaseous and liquid clath-

[†] Department of Chemistry, University of California at Davis.
[‡] Department of Chemical Engineering and Materials Science, University of California at Davis.
[§] National Center of Electron Microscopy, Lawrence Berkeley Laboratory.
[||] NMR Facility, University of California at Davis.
[⊥] Materials Science and Technology Division, Lawrence Livermore National Laboratory.

(1) Fichtner, M. *Adv. Eng. Mater.* **2005**, *7*, 443−455.
(2) Banerjee, S.; Murad, S.; Puri, I. K. *Proc. IEEE* **2006**, *94*, 1806−1814.
(3) Chu, X. Z.; Zhou, Y. P.; Zhang, Y. Z.; Su, W.; Sun, Y.; Zhou, L. *J. Phys. Chem. B* **2006**, *110*, 22596−22600.
(4) Chen, B. L.; Ockwig, N. W.; Millward, A. R.; Contreras, D. S.; Yaghi, O. M. *Angew. Chem., Int. Ed.* **2005**, *44*, 4745−4749.
(5) Rosi, N. L.; Eckert, J.; Eddaoudi, M.; Vodak, D. T.; Kim, J.; O'Keeffe, M.; Yaghi, O. M. *Science* **2003**, *300*, 1127−1129.
(6) Dinca, M.; Long, J. R. *J. Am. Chem. Soc.* **2005**, *127*, 9376−9377.
(7) Dinca, M.; Yu, A. F.; Long, J. R. *J. Am. Chem. Soc.* **2006**, *128*, 8904−8913.
(8) Li, Y. W.; Yang, R. T. *J. Phys. Chem. B* **2006**, *110*, 17175−17181.
(9) Palomino, G. T.; Carayol, M. R. L.; Arean, C. O. *J. Mater. Chem.* **2006**, *16*, 2884−2885.
(10) Nechaev, Y. S. *Phys.-Usp.* **2006**, *49*, 563−591.
(11) Gogotsi, Y.; Dash, R. K.; Yushin, G.; Yildirim, T.; Laudisio, G.; Fischer, J. E. *J. Am. Chem. Soc.* **2005**, *127*, 16006−16007.
(12) Florusse, L. J.; Peters, C. J.; Schoonman, J.; Hester, K. C.; Koh, C. A.; Dec, S. F.; Marsh, K. N.; Sloan, E. D. *Science* **2004**, *306*, 469−471.

rates hydrates crystallize in seven structural types, types I−VII. The crystal structure of any clathrate consists of a three-dimensional host framework. The cavities or cages in the framework are polyhedra with pentagonal and hexagonal faces that can encapsulate guest atoms. These cages can be denoted as $[5^{12}]$ for a pentagonal dodecahedron, $[5^{12}6^2]$ for a tetrakaidecahedron, $[5^{12}6^3]$ for a pentakaidecahedron, and $[5^{12}6^4]$ for a hexakaidecahedron.[13] The main feature of these phases is the almost nonexistent chemical interaction between the molecules of the host matrix (H_2O) and the molecules occupying the cavities. Typical guest molecules found in the hydrate clathrate phases are CO_2, Cl_2, CH_4, and other light hydrocarbons. Similar to the MOFs, the clathrates allow for significant flexibility in the cage or pore dimension as a function of the host structure. For example, a clathrate hydrate was found to uptake 6.5% hydrogen under extreme pressures (2 kbar) at 77 K.[14] Moreover, it has been reported that those extreme conditions can be altered by simply allowing the larger cages of the clathrate structure to be occupied by tetrahydrofuran (THF) guest molecules.[15] High-resolution neutron diffraction studies of deuterium substituted hydrate clathrates have shown that the small cavity of the THF hydrate is occupied by one deuterium molecule.[12] However, it is expected that the appropriate formation conditions may allow for higher storage capacity in a material, which is essentially composed of only water and hydrogen.

Silicon clathrates, similar to their hydrate counterparts, are made of the silicon host framework that can exist either empty or filled with electron-donating guest atoms such as alkali or alkaline earth metals.[16] The observation of superconductivity and "phonon glass-electron crystal" behavior leading to promising thermoelectric materials, as well as theoretically predicted large band gaps in the guest-free clathrate structures, Si_{34}, and Si_{46}, has renewed the interest in these compounds.[17−19] This work adds another important application for these materials, namely hydrogen storage.

The most studied silicon clathrate structures are types I and II. Figure 1 shows the crystal structure of a type I silicon clathrate. Type I clathrates crystallize in the cubic system of the centrosymmetrical space group $Pm\bar{3}n$, and they have two crystallographically distinct guest sites (*2a* and *6d*) and three Si framework sites (*6c*, *16i*, and *24k*) giving the general formula A_8Si_{46}. Type I silicon clathrate structure contains two types of polyhedra, a pentagonal dodecahedron, denoted as $[5^{12}]$ and a tetrakaidecahedron, $[5^{12}6^2]$. The $[5^{12}]$ unit constitutes the Si_{20} cage, and it is a 20 vertex polyhedron containing 12 pentagonal faces, thus the notation 5^{12}. The $[5^{12}6^2]$ constitutes a Si_{24} cavity, and it is a 24-vertex polyhedron with 12 pentagonal and 2 hexagonal faces. In general, type I silicon clathrates, A_8Si_{46} (A = Na, K, Rb, Cs), can be formed under vacuum or inert-atmosphere conditions from the controlled thermal decomposition of the corresponding Zintl salt ASi.[20−23] The reaction takes place at 350−450 °C and produces a mixture of types II and I clathrates, A_xSi_{136} and A_8Si_{46}, respectively. The mixture of types II and I clathrates can be further separated by density methods.[22] Empty and cation deficient type II clathrates of both germanium and silicon have been reported and characterized.[22,24] Type I silicon clathrates that are cation deficient have been also reported for the larger cations potassium and rubidium and also for the sodium barium superconductive alloys.[18,23,25]

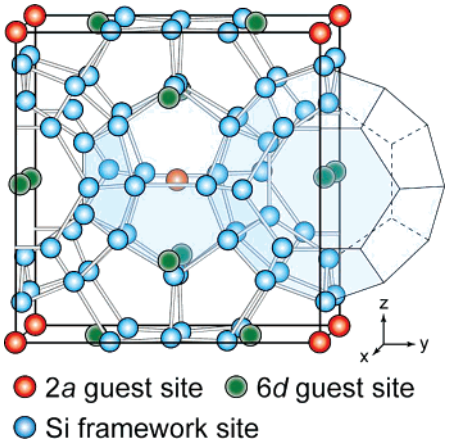

Figure 1. View of the type I clathrate structure, Na_8Si_{46}. Guest atoms: in *2a* site, red; in *6d* site, green. Silicon framework atoms = light blue. The two types of Si cages are indicated.

Herein we report the formation of a sodium-deficient type I silicon clathrate, $Na_{5.5}(H_2)_{2.15}Si_{46}$, in high yield utilizing a novel synthetic procedure. We show that the silicon framework has entrapped hydrogen molecules and that it is stable at ambient temperature and pressure. This work describes the first member of this new type I sodium-deficient hydrogen-containing silicon clathrate, along with the structural characterization of this compound. We propose that more hydrogen rich species may be discovered in these unique clathrate structures.

Experimental Section

1. Synthesis. All manipulations for the synthesis of the silicon clathrate were performed in a N_2-filled glovebox or vacuum/inert atmosphere Schlenk line. Silicon (99.999%, Aldrich) and sodium (lump 99%, Aldrich) were used as received. Sodium silicide was prepared according to literature methods,[26] and the purity was confirmed by powder X-ray diffraction. Ammonium bromide (99.99%, Aldrich) was dried under dynamic vacuum at 100 °C for 14 h prior usage. The clathrate, $Na_{5.5}(H_2)_{2.15}Si_{46}$, was obtained by the solid-state reaction between the Zintl salt, NaSi, and ammonium bromide. A 1:1 molar ratio of the two solid reactants was ground in an agate mortar in a nitrogen-filled glovebox, and the resulting powder was pressed into pellets. The pellets were then introduced in an oven preheated at 300 °C under dynamic vacuum for 12 h. The clathrate phase was separated from the salt byproduct by washing first with ethanol and then with

(13) Kovnir, K. A.; Shevelkov, A. V. *Usp. Khim.* **2004**, *73*, 999−1015.
(14) Lee, H.; Lee, J. W.; Kim, D. Y.; Park, J.; Seo, Y. T.; Zeng, H.; Moudrakovski, I. L.; Ratcliffe, C. I.; Ripmeester, J. A. *Nature* **2005**, *434*, 743−746.
(15) Strobel, T. A.; Taylor, C. J.; Hester, K. C.; Dec, S. F.; Koh, C. A.; Miller, K. T.; Sloan, E. D. *J. Phys. Chem. B* **2006**, *110*, 17121−17125.
(16) Kasper, J. S.; Hagenmuller, P.; Pouchard, M.; Cros, C. *Science* **1965**, *150*, 1713−14.
(17) Iversen, B. B.; Palmqvist, A. E. C.; Cox, D. E.; Nolas, G. S.; Stucky, G. D.; Blake, N. P.; Metiu, H. *J. Solid State Chem.* **2000**, *149*, 455−458.
(18) Yamanaka, S.; Kawaji, H.; Ishikawa, M. In *Cluster Assembled Materials*; Trans Tech Publications: Switzerland, 1996; Vol. 232, pp 103−117.
(19) Tanigaki, K.; Shimizu, T.; Itoh, K. M.; Teraoka, J.; Moritomo, Y.; Yamanaka, S. *Nat. Mater.* **2003**, *2*, 653−655.
(20) Tse, J. S.; Uehara, K.; Rousseau, R.; Ker, A.; Ratcliffe, C. I.; White, M. A.; MacKay, G. *Phys. Rev. Lett.* **2001**, *86*, 4980−4980.
(21) Bobev, S.; Sevov, S. C. *J. Solid State Chem.* **2000**, *153*, 92−105.
(22) Ramachandran, G. K.; Dong, J. J.; Diefenbacher, J.; Gryko, J.; Marzke, R. F.; Sankey, O. F.; McMillan, P. F. *J. Solid State Chem.* **1999**, *145*, 716−730.
(23) Ramachandran, G. K.; McMillan, P. F. *J. Solid State Chem.* **2000**, *154*, 626−634.
(24) Guloy, A. M.; Ramlau, R.; Tang, Z. J.; Schnelle, W.; Baitinger, M.; Grin, Y. *Nature* **2006**, *443*, 320−323.
(25) Bohme, B.; Guloy, A.; Tang, Z. J.; Schnelle, W.; Burkhardt, U.; Baitinger, M.; Grin, Y. *J. Am. Chem. Soc.* **2007**, *129*, 5348.
(26) Mayeri, D.; Phillips, B. L.; Augustine, M. P.; Kauzlarich, S. M. *Chem. Mater.* **2001**, *13*, 765−770.

HPLC grade water. The resulting dark gray powder was dried under flowing argon at 80−100 °C overnight. The solid products were characterized by powder X-ray diffraction.

2. Characterization. Elemental Analysis. Elemental analysis was performed on three different reaction batches by Galbraith[27] and Desert Analytics Laboratories.[28] These gave the Na:Si ratio 5.6:46 (H was not determined) and the Na:Si:H ratios of 5.2:46:4 and 5.8:46:4.6. Averaging these three measurements provides the approximate formula $Na_{5.5}(H_2)_{2.15}Si_{46}$. A small amount of NaBr was also observed in the samples, and the molar amounts were removed from the totals. Total weight percent did not add to 100%, so to better characterize the composition, X-ray energy dispersive spectroscopy (EDX) was employed in a TEM measurement described below. EDX data provided a ratio of 4.7:46 for Na:Si, and no other elements were detected.

Powder X-ray Diffraction. Powder X-ray diffraction (XRD) studies were carried out on an Inel (Co Kα radiation, $\lambda = 1.788\ 97$ Å). Data were collected in a continuous scan mode between 10 and 115° in 2θ with a step size of 0.03. Structural refinement by the Rietveld method was performed using the program Rietica.[29] The refined parameters include background, peak shape, cell, atom positions, scale factor, thermal parameters, and occupancies. The R-factor (R_p), the weighted R-factor (wR_p), and the goodness of fit, χ^2, are defined as follows: $R_p = \Sigma[y_{io} - y_{ic}]/\Sigma y_{io}$, $wR_p = [\Sigma w_i(y_{io} - y_{ic})^2/\Sigma w_i(y_{io})^2]^{1/2}$, and $\chi^2 = [wR_p/R_{exp}]^2$, where $R_{exp} = [(N - P)/\Sigma w_i y_{io}^2]^{1/2}$ and y_{io} and y_{ic} are the observed and the calculated intensities, w_i is the weighting factor, N is the total number of observed intensities when the background is refined, and P is the number of adjusted parameters.

Solid-State NMR. For all solid-state NMR work approximately 150 mg of sample was loaded in a Bruker zirconia rotor with kel-F caps in a glovebox filled with dry flowing nitrogen. Solid-state NMR experiments were performed on a Bruker Avance 500 spectrometer equipped with an 11.75 T magnet and a Bruker 4 mm CPMAS probe. The magic angle spinning (MAS) rate was 15 kHz. A solid-echo pulse sequence (90−t−90−acquisiton) was used to suppress the ring-down of the probe for the ^{23}Na MAS NMR spectrum. The 90 deg pulse width was 1.5 μs, the interpulse delay time (t) was synchronized with rotor time, the spectrum width was 2.5 MHz, the relaxation delay was 0.5 s, a total of 12 000 transients were averaged, and a block size of 16384 was recorded and processed with 100 Hz line broadening. For ^{1}H MAS NMR, a Hahn echo pulse sequence (90−t−180−acquisiton) was used to suppress the signal from the probe background. The 90 deg pulse width was 2.5 μs, the interpulse delay time (t) was synchronized with rotor time, the spectrum width was 500 kHz, the relaxation delay was 5 s, a total of 2000 transients were averaged, and a block size of 8192 was used and zero-filled to 16 384 with 1 Hz line broadening. The ^{29}Si MAS NMR experiment was conducted on the same spectrometer equipped with a Bruker 7 mm CP-MAS probe with a MAS rate of 6 kHz. The 90-deg pulse width was 4 us, the relaxation delay was 1 s, the spectrum width was 250 kHz, a total of 235 148 transients were averaged, and a block size of 8192 was recorded and processed with 100 Hz line broadening.

FTIR. FTIR data was obtained using a Shimadzu IR Prestige 21 equipped with a diffusive reflectance accessory. The powder was mixed with the KBr using a 1:100 molar ratio dilution of the sample in the KBr matrix. The samples were mixed with KBr in a nitrogen-filled drybox and then loaded in vials and brought out of the drybox just before the measurement. The IR measurements were performed in air.

EDX/SAED/STEM. Approximately 0.1 g of the synthesized powder was sonicated for 30 min in *n*-butanol and spread over a gold-mesh grid covered by a thin perforated carbon film. The grid was heated in air at 200 °C overnight. Selected area electron diffraction (SAED) and energy dispersive X-ray spectroscopy (EDX) were performed under JEOL JEM-2500SE electron microscope operated at 200 kV. The sample was also examined using spherical aberration (Cs) corrected VG HB501 scanning transmission electron microscope (STEM) operated at 100 kV. High-angle annular dark-field (HAADF) images were taken along [100] with the convergence semiangle of 20 mrad and collection semiangle of 70−210 mrad. STEM image calculation was made with Kirkland's code.[30]

Results and Discussion

Most silicon-containing clathrate phases are prepared either by high-temperature methods involving the elements or by vacuum thermal decomposition of NaSi. In a recent publication on the use of ammonium halides to prepare photoluminescent silicon and germanium from metal silicides and germanides, it was noted that diffraction peaks associated with the clathrate structure were present in the powder patterns as impurities.[31] Independently, while developing the synthetic methodology to prepare macroscopic amounts of hydrogen-capped silicon nanoparticles,[32] we discovered that silicon type I clathrate could be prepared in high yield and purity by heating the reaction mixture under dynamic vacuum at 300 °C. The reaction scheme between the Zintl salt, NaSi, and ammonium halide is shown as

$$46NaSi + 40.5NH_4Br \rightarrow Na_{5.5}(H_2)_{2.15}Si_{46} + 40.5NaBr + 40.5NH_3 + 18.1H_2 \quad (1)$$

The powder X-ray diffraction pattern, shown in Figure 2, of the product is consistent with type I clathrate structure (Figure 1), and the diffraction peaks were indexed to a cubic cell, space group $Pm\bar{3}n$, $a = 10.1944(5)$ Å. The cell parameters are listed in Table 1. The crystal structure data obtained from the refinement are in good agreement with the reported values in literature.[22] The cubic cell is only slightly smaller than the value reported for a fully sodium occupied clathrate, Na_8Si_{46}, $a = 10.19648(2)$ Å.[22] The occupancies of sodium were allowed to refine. The values are reported in Table 1 giving a total of 1.728 Na for the *2a* position and 5.616 Na for the *6d* position, suggesting that there was Na deficiency in both sites. Elemental analysis on this material provided even a lower amount of Na and was consistent with the formula $Na_{5.5}(H_2)_{2.15}Si_{46}$. The Rietveld refinement may provide higher than expected Na content because of the correlation between thermal and occupancy parameters. Other factors, such as background, absorption, extinction, etc., also can contribute to errors in occupancy refinement.[33]

Solid-state ^{23}Na, ^{1}H, and ^{29}Si MAS NMR data provide further information about the structure of this new compound. Figure 3 displays the solid-state ^{23}Na MAS NMR spectrum. A small amount of remaining NaBr salt was also present in the ^{23}Na NMR spectrum (near 0 ppm; data not shown here). The two peaks observed are consistent with the two characteristic Knight shifts for the Na atom in a Si_{20} cage (*2a* crystallographic site) at ∼2018 ppm and for the Na in the Si_{24} cage (*6d* crystallographic site) at ∼1730 ppm.[34,35] The observed Knight shifts are quite high, even higher than for metallic sodium, 1131

(27) http://www.galbraith.com/.
(28) http://www.desertanalytics.com/index.htm.
(29) www.rietica.org.

(30) *Advanced Computing in Electron Microscopy*; Kirkland, E. J., Ed.; Plenum Press: New York, 1998.
(31) McMillan, P. F.; Gryko, J.; Bull, C.; Arledge, R.; Kenyon, A. J.; Cressey, B. A. *J. Solid State Chem.* **2005**, *178*, 937−949.
(32) Neiner, D.; Chiu, H. W.; Kauzlarich, S. M. *J. Am. Chem. Soc.* **2006**, *128*, 11016−11017.
(33) Yamazaki, S.; Toraya, H. *J. Appl. Crystallogr.* **1999**, *32*, 51−59.
(34) Gryko, J.; McMillan, P. F.; Sankey, O. F. *Phys. Rev. B* **1996**, *54*, 3037−3039.
(35) Pouchard, M.; Cros, C.; Hagenmuller, P.; Reny, E.; Ammar, A.; Menetrier, M.; Bassat, J. M. *Solid State Sci.* **2002**, *4*, 723−729.

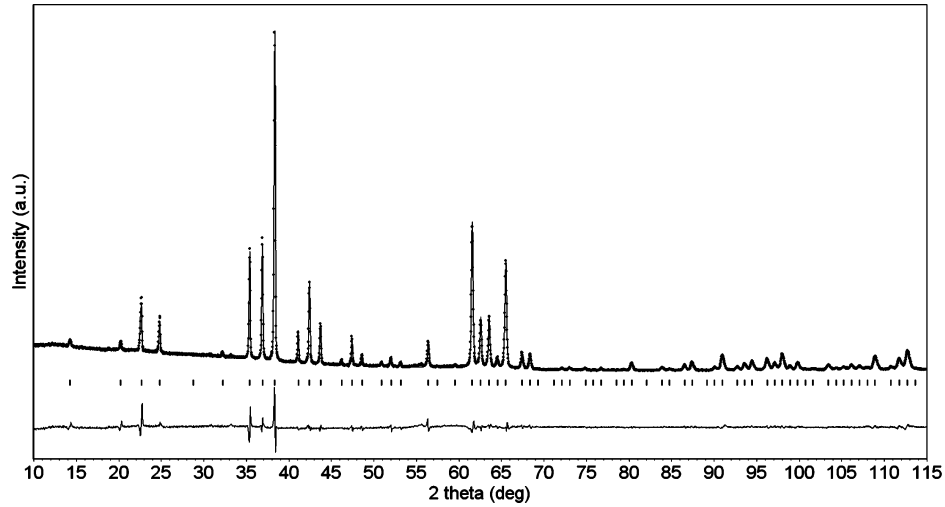

Figure 2. Rietveld profile fit for the sodium clathrate prepared in this study. Experimental data points are shown as black crosses, and the theoretical fit is shown as a black solid curve. The data were refined for the space group $Pm\bar{3}n$ (upper black ticks), and the difference between the observed and theoretical patterns is shown below the black ticks. The unit cell is $a = 10.1944(5)$ Å, with $R_p = 5.259\%$, $R_{wp} = 7.178\%$, and $\chi^2 = 8.669$.

Table 1. Atomic Coordinates and Equivalent Isotropic Displacement Parameters (U_{eq})[a] for the Clathrate Phase Prepared in This Paper

atom	site	*x*	*y*	*z*	U_{eq} (Å^2)	occupancy
$Na_{5.5}(H_{2.15})_2Si_{46}$						
Na(1)	*2a*	0	0	0	0.0125(3	0.864(1)
Na(2)	*6d*	0	0.25	0.5	0.0204(2)	0.936(1)
Si(1)	*6c*	0.25	0	0.5	0.0108(8)	1
Si(2)	*16i*	0.1840(2)	0.1840(2)	0.1840(2)	0.0115(5)	1
Si(3)	*24k*	0. 1177(2)	0	0.3084(2)	0.00970(4)	1

[a] U_{eq} is defined as one-third of the trace of the orthogonalized $\mathbf{U}_{ij}$ tensor.

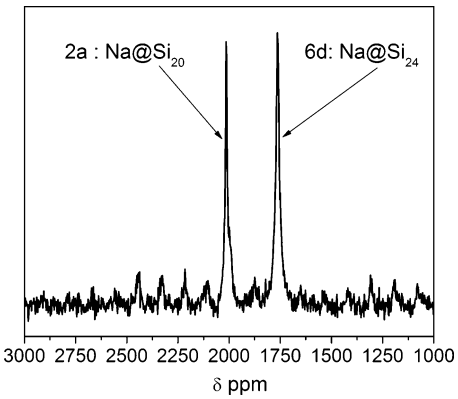

Figure 3. Magic angle spinning ^{23}Na solid-state NMR spectrum for $Na_{5.5}(H_2)_{2.15}Si_{46}$. The two main resonances correspond to the guest crystallographic sites, *2a* and *6d*. Sodium in the *2a* site is in the Si_{20} cage, and sodium in the *6d* site is in the Si_{24} cage. A small signal corresponding to NaBr is also present, data not shown.

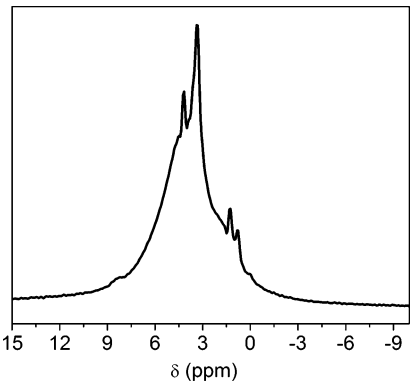

Figure 4. Magic angle spinning ^{1}H solid-state NMR spectrum for $Na_{5.5}(H_2)_{2.15}Si_{46}$.

ppm,[36] showing that sodium has transferred approximately 10% of its electron density to the silicon framework.[34−36] These large values have been explained as arising from the nuclear hyperfine interaction with the unpaired electrons.[36] The assignment of these resonances are consistent with the literature assignments reported for the fully occupied Na_8Si_{46} type I clathrate structure.[34−36] The integrated intensities of the two isotropic peaks[36] give a 1:1.5 ratio for the *2a*:*6d* crystallographic sites. According to this ratio, if one assumes that the *2a* crystallographic site is fully occupied with 2 Na atoms, then the large *6d* site can only contain 3 Na. This suggests that the large cages (*6d* site), Si_{24}, are Na deficient, which is consistent with the elemental analysis and the EDX results of $Na_{5.5}Si_{46}$. Deficiency of the Na from the large cage for Na_8Si_{46} has been noted previously and was attributed to the exact details of the preparation.[36]

The solid-state ^{1}H MAS NMR spectrum is presented in Figure 4. There are five distinct resonances in the ^{1}H NMR spectrum at 4.2, 3.8, 1.3, 0.79, and 0.08 ppm. Proton solid-state NMR has been reported on a type II THF·H_2O clathrate, which under hydrogen pressure can store up to 1 wt % H_2.[14,15] The authors proposed that the hydrogen in the small cages (X_{20}) gives rise to the resonance at ~4.2 ppm and that hydrogen in the large cages (X_{28}) gives rise to the resonance at about 0 ppm.[14,15] Our spectrum is very similar to theirs with a resonance at about 4.2 ppm. However, the ^{1}H MAS NMR spectrum presented here is more complicated than the hydrate one, showing sharp reso-

(36) He, J. L.; King, D. D.; Uehara, K.; Preston, K. F.; Ratcliffe, C. I.; Tse, J. S. *J. Phys. Chem. B* **2001**, *105*, 3475−3485.

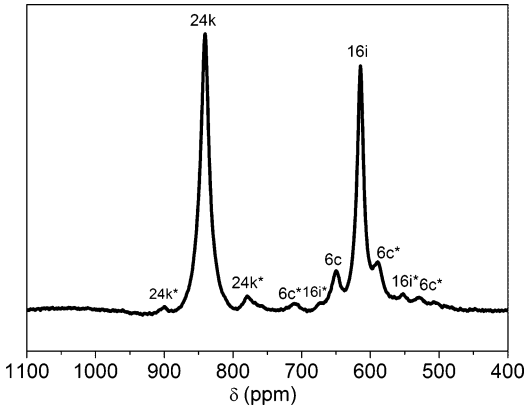

Figure 5. Magic angle spinning ^{29}Si solid-state NMR spectrum for $Na_{5.5}(H_2)_{2.15}Si_{46}$. The isotropic shifts are assigned to the three silicon crystallographic sites as indicated.

nances along with the broad resonance. The narrow line widths are consistent with a hydrogen molecule that can freely rotate in the cavities, and the broad resonance is more consistent with hydrogen that has more restricted motion and may be interacting with the cages. The assignment of these peaks to hydrogen molecules rather than hydrogen covalently bound to silicon is consistent with the absence of any Si−H stretches in the FTIR. The hydrogen molecule that gives rise to 4.2 ppm resonance is assigned to the large Si_{24} cage. This is a reasonable assignment since the ^{23}Na NMR shows that the Si_{24} cage is deficient in Na and the 4.2 ppm resonance is similar to that observed in the hydrate clathrate[14,15] and to hydrogen molecules trapped in the 5^{12} cages of microporous crystalline silica.[37] These chemical shifts are quite different from the ones found in hydrogen encapsulated fullerenes derivatives, presumably because of the very different chemical environments.[38,39] The ^{1}H resonances do not appear to be "Knight shifted" unlike the Na resonances. This suggests that there is negligible electron density transfer from the hydrogen molecule to the silicon framework. The hydrogen molecule, with its covalent bond, is significantly less electropositive than Na and would be less likely to transfer electron density to the framework.

The solid-state ^{29}Si MAS NMR spectrum, presented in Figure 5, is consistent with a clathrate type I structure. There are three crystallographic silicon sites (*16i*, *6c*, and *24k*) that can be assigned to the three distinct Knight-shifts, at ∼617 ppm for the silicon in the *16i* site, at ∼653 ppm for the Si in *6c*, and ∼842 ppm for the Si in the *24k* site. These values are in agreement with literature values for Na_8Si_{46} with a silicon framework of a type I clathrate structure.[35,36,40] The resonances are labeled according to their crystallographic site symmetry. The integrated intensities under the main peaks and their associated spinning side bands gave the following silicon occupancies ratios over the three different crystallographic sites: Si in *24k* is 24, Si in *16i* is 15.8, and Si in *6c* is 7.5. These results are consistent with the stoichiometry of Si_{46} with all the framework sites completely filled.[36]

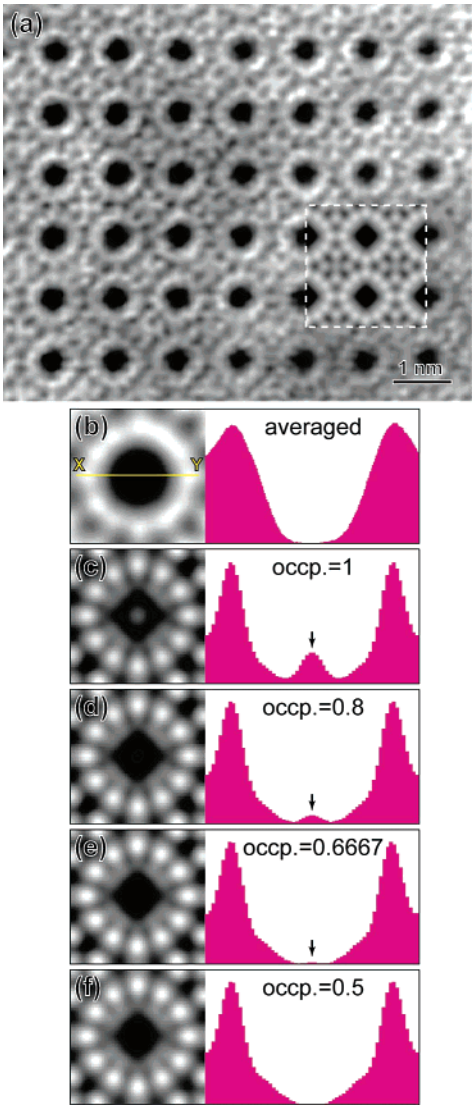

Figure 6. (a) STEM-HAADF image of $Na_{5.5}(H_{2.15})_2Si_{46}$ taken along the [100] direction. The calculated image of 2 × 2 unit cells is inserted. (b) Averaged experimental image and intensity profile along the line *x*−*y*. (c-f) Calculated images with different Na occupancies in the 6*d* sites and intensity profiles.

Further characterization was obtained for this material by EDX, SAED, and STEM. Although a hollow electron diffraction pattern due to an amorphous structure, also present in the X-ray powder diffraction pattern background, was observed for a small number of particles, the SAED patterns observed for most particles of the sample correspond to those of the type I clathrate structure without any superlattice reflections, indicating that the Na atoms are disordered in the guest atom sites. EDX supports the elemental analysis data, and the ^{23}Na NMR data for that sodium/silicon ratio indicate Na:Si = 4.7:46 and did not show the presence of Br. ^{23}Na NMR data show the presence of NaBr that is not apparent from the TEM grids, presumably because of the differences in size of sample and how the samples are prepared for these two different techniques. The NMR sample is a large sample size (150 mg) whereas the TEM sample is a very small sample that is suspended in a solvent before deposition on the grid. Presumably, the small amount of NaBr observed by NMR does not deposit on the grid along with the clathrate sample. Figure 6a shows a HAADF-STEM image taken

(37) Van den Berg, A. W. C.; Pescarmona, P. P.; Schoonman, J.; Jansen, C. J. *Chem.—Eur. J.* **2007**, *13*, 3590−3595.
(38) Murata, Y.; Murata, M.; Komatsu, K. *J. Am. Chem. Soc.* **2003**, *125*, 7152−7153.
(39) Iwamatsu, S.; Murata, S.; Andoh, Y.; Minoura, M.; Kobayashi, K.; Mizorogi, N.; Nagase, S. *J. Org. Chem.* **2005**, *70*, 4820−4825.
(40) Ramachandran, G. K.; McMillan, P. F.; Diefenbacher, J.; Gryko, J.; Dong, J. J.; Sankey, O. F. *Phys. Rev. B* **1999**, *60*, 12294−12298.

along [100]. The image was calculated with a thickness of 21 nm and defocus value of 22.5 nm. The calculated image inserted in Figure 6a is in good agreement with the experimental one. The ring pattern and the center of the ring correspond to the Si_{24} cage and the *6d* sites, respectively. When observed along [100], the *6d* sites are aligned in an atomic column, which is apart from the nearest columns by 0.23 nm so that the Na occupancy in the *6d* sites can be determined by comparing the experimental intensity profiles with calculated ones. Figure 6b−f shows an averaged experimental image using 2dx software and calculated images with different Na occupancies in the 6*d* sites as well as intensity profiles along the line $x-y$.[41] The peak intensity at the 6*d* sites decreases with the decreasing Na occupancy as indicated by arrows in the intensity profiles, and no peak is observed when the occupancy reaches 0.5. This indicates that more than one-third of Na in the *6d* sites is deficient, which is consistent with both ^{23}Na NMR and elemental analysis data.

Summary

We present a simple low-temperature synthetic route to a nearly phase pure type I clathrate of silicon that encapsulates hydrogen molecules in the cages at ambient temperatures and pressures. Powder X-ray diffraction data and SAED are consistent with the type I silicon clathrate structure. Silicon NMR confirms the presence of silicon in the three clathrate framework sites as being fully occupied. Sodium NMR, HAADF-STEM, and elemental analysis are consistent with sodium deficiency in large *6d* cages. Sodium deficiency would allow hydrogen to fill the remainder of the cavities in this compound. Proton NMR and elemental analysis shows the presence of hydrogen in this compound. It may be possible, through synthetic optimization, to increase the amount of hydrogen present and to prepare other clathrate structures. With simple variations of the identity of the metals in the metal silicide, along with alternative temperature profiles for the reaction described herein, more hydrogen-rich species are yet to be discovered in these unique clathrate structures.

Acknowledgment. We gratefully acknowledge Dr. Alexandra Navrotsky (Department of Chemistry and Thermochemistry Facility and NEAT ORU, University of California, Davis, CA) for use of the Inel powder diffractometer. We wish to thank David G. Morgan, who carried out the image processing using 2dx software. This work was supported by the Center of Excellence for Chemical Hydrides under Contract No. DE-FC36-05GO15055, by the Department of Energy under Contract No. DE-FG02-03ER46057, and by the Japan Society for the Promotion of Science for Young Scientists. C.L.C. acknowledges a Tyco Electronics Foundation Fellowship in functional materials.

JA0724700

(41) Gipson, B.; Zeng, X.; Zhang, Z. Y.; Stahlberg, H. *J. Struct. Biol.* **2007**, *157*, 64−72.